J Physiol (2003), **553.1**, *pp.* 113–123

DOI: 10.1113/jphysiol.2003.043034
www.jphysiol.org

Journal of Physiology

Voltage-gated Na^+ channel activation induces both action potentials in utricular hair cells and brain-derived neurotrophic factor release in the rat utricle during a restricted period of development

Christian Chabbert, Ilana Mechaly, Victor Sieso, Pierre Giraud*, Aurore Brugeaud, Jacques Lehouelleur, François Couraud*, Jean Valmier and Alain Sans

*INSERM U583, UM2 cc089, place E. Bataillon, 34095 Montpellier cedex 5, and *INSERM U464, Université de la Méditerranée, Institut Jean Roche, Bd Pierre Dramard, 13916 Marseille cedex 20, France*

The mammalian utricular sensory receptors are commonly believed to be non-spiking cells with electrical activity limited to graded membrane potential changes. Here we provide evidence that during the first post-natal week, the sensory hair cells of the rat utricle express a tetrodotoxin (TTX)-sensitive voltage-gated Na^+ current that displays most of the biophysical and pharmacological characteristics of neuronal Na^+ current. Single-cell RT-PCR reveals that several α-subunit isoforms of the Na^+ channels are co-expressed within a single hair cell, with a major expression of Nav1.2 and Nav1.6 subunits. In neonatal hair cells, 30 % of the Na^+ channels are available for activation at the resting potential. Depolarizing current injections in the range of the transduction currents are able to trigger TTX-sensitive action potentials. We also provide evidence of a TTX-sensitive activity-dependent brain-derived neurotrophic factor (BDNF) release by early post-natal utricle explants. Developmental analysis shows that Na^+ currents decrease dramatically from post-natal day 0 (P0) to P8 and become almost undetectable at P21. Concomitantly, depolarizing stimuli fail to induce both action potential and BDNF release at P20. The present findings reveal that vestibular hair cells express neuronal-like TTX-sensitive Na^+ channels able to generate Na^+-driven action potentials only during the early post-natal period of development. During the same period an activity-dependent BDNF secretion by utricular explants has been demonstrated. This could be an important mechanism involved in vestibular sensory system differentiation and synaptogenesis.

(Received 14 March 2003; accepted after revision 4 September 2003; first published online 5 September 2003)
Corresponding author A. Sans: INSERM U583, Université Montpellier II, Place Eugène Bataillon, cc 089, 34095 Montpellier cedex 5, France. Email: alansans@univ-montp2.fr

During development, immature neurons of the central nervous system generate an electrical activity (i.e. action potentials and synaptic potentials) that drives activity-dependent processes including neuronal survival and differentiation, establishment of connectivity and synapse stabilization (Katz & Shatz, 1996). A growing body of evidence indicates that the neurotrophin gene family may mediate some of the effects of neuronal activity in regulating neuron–neuron interactions (Thoenen, 1995). The activity-dependent regulation of neurotrophins has been shown to control survival of cortical neurons (Ghosh *et al.* 1994), neuronal synaptogenesis and plasticity (Kafitz *et al.* 1999), differentiation of neuronal phenotype (Boukhaddaoui *et al.* 2001) and potentiation of neurotransmitter release (Stoop & Poo, 1996; Goggi *et al.* 2002).

Utricular hair cells are non-neuronal sensory receptors whose direct interaction with their primary sensory neurons is required for harmonious development and adult functioning of the vestibular system (Fritzsch *et al.* 2001). The mammalian vestibular sensory receptors were commonly assumed to be non-spiking cells with electrical activity limited to graded membrane potential changes. It is now well established that utricular hair cells express a complex and developmentally regulated pattern of voltage-gated K^+ and Ca^{2+} currents (Eatock & Rusch 1997; Rusch *et al.* 1998). Recent data indicate that mouse and rat utricular hair cells also express voltage-gated Na^+ currents, I_{Na} (Rusch & Eatock 1997; Lennan *et al.* 1999), raising the possibility that their activation may be able to generate action potentials. Developing hair cells and supporting cells

C. Chabbert and I. Mechaly contributed equally to this study

synthesize brain-derived neurotrophic factor (BDNF) and neurotrophin-3 (NT3), two members of the neurotrophin gene family. Moreover their innervating sensory neurons express BDNF and NT-3 high-affinity receptors, respectively TrkB and TrkC (Pirvola *et al.* 1992, 1994). Both neurotrophins and their receptors are required for the survival of sensory neurons (Schimmang *et al.* 1995; Ernfors *et al.* 1995; Fritzsch *et al.* 1997; Montcouquiol *et al.* 1997), and an important role for BDNF in the maturation of the synapse between afferent neurons and vestibular hair cells has been suggested (Montcouquiol *et al.* 1998).

To check the involvement of I_{Na} in generating electrical activity, we undertook patch-clamp recordings in the rat utricle hair cells using the voltage- and current-clamp configurations during the first post-natal week. We used ELISA *in situ* to study whether hair cell neurotrophin is released by an activity-dependent mechanism. We demonstrated that: (i) neonatal rat utricle hair cells express a neuronal-like tetrodotoxin (TTX)-sensitive I_{Na} with biophysical properties compatible with a spiking activity; (ii) TTX-sensitive action potentials could be evoked upon injection of a depolarizing current in the range of transduction currents; (iii) electrical stimulations of neonatal utricle explants induce TTX-sensitive BDNF release. I_{Na}, TTX-sensitive action potentials and activity-dependent BDNF release disappear when synaptogenesis is completed.

METHODS

Electrophysiological recordings

Embryos and early post-natal (post-natal day (P)0–P3) rats were killed by decapitation. Post-natal and adult rats were deeply anaesthetized with CO_2 and then decapitated. Procedures involving animals and their care were conducted in agreement with the French Ministry of Agriculture and the European Community Council Directive no. 86/609/EEC, OJL 358, 18 December 1986. Utricular maculae were acutely dissected from Wistar rats between embryonic day 20 (E20) (1 day before birth) and P21, and mounted for electrophysiological studies as previously described (Lennan *et al.* 1999). Epithelia were placed in an experimental chamber containing 2 ml of external control solution (mM: 137 NaCl, 0.7 NaH_2PO4, 5.8 KCl, 1.3 $CaCl_2$, 0.9 $MgCl_2$, 5.6 D-glucose, 10 Hepes-NaOH, pH 7.5; amino acids and vitamins for Eagle's MEM were added from concentrates, Gibco, UK). The chamber was continuously superfused at 1 ml min^{-1} using a peristaltic pump. Transverse cuts were performed close to the edge of the macula to ascertain that the recorded cells were at approximately the same stage of development, since there is a gradient of maturity from the centre towards the periphery in this organ (Sans & Chat, 1982). Prior to P4, hair cells are referred to as immature cells, as the acquisition of electrophysiological criteria that discriminate between the two types of hair cells – type I and type II – occurs only from P4 in the mouse utricle (Rusch *et al.* 1998). In the rat, I_{Na} was not detected from P4 in cells that exhibited criteria previously described as 'type I category'. No enzymatic treatment was used.

After seal formation (>10 GΩ) onto the basolateral membrane of hair cells and membrane disruption, the membrane capacitance (C_m) and series resistance (R_s) were estimated from the decay of the capacitive transient induced by a ±10 mV pulse from a holding potential of −100 mV. R_s values were in the range of 4–11 MΩ and C_m (5.2 ± 1.1 pF; $n = 112$) could be charged with a time constant around 100 μs. R_s values were compensated for up to 85% after cancellation of the capacitive transients. Voltage errors resulting from uncompensated R_s never exceeded 5 mV and were not corrected. No linear leakage compensation was performed. Voltages were corrected off-line for liquid junction potentials measured according to Neher (1992): −2 mV between internal and external control solutions, −5 mV between the internal caesium solution and the external TEA solution, and −10 mV measured between the internal potassium gluconate solution and the external control solution. Voltage steps were applied to the cell membrane and whole-cell currents were recorded under voltage-clamp using an Axopatch 200B patch-clamp amplifier (Axon Instruments, Union City, CA, USA). Data were sampled at 5 or 10 kHz (pCLAMP6, Axon Instruments) and filtered at half the sampling rate (8-pole Bessel filter). For voltage-clamp recordings, patch pipettes (2–4 MΩ) contained an internal control solution (mM): 135 KCl, 0.1 $CaCl_2$, 5 EGTA, 3 MgATP, 1 NaGTP, 5 Hepes-NaOH, pH 7.3. Characterization of the I_{Na} was performed in isolation in P0–P2 hair cells, by substituting 135 mM Cs^+ for K^+ in the internal solution, and 50 mM TEA for Na^+ in the external solution. Examination of the presence of I_{Na} over time and current-clamp recordings were performed using internal and external control solutions. In some current-clamp experiments a low Cl^- internal solution, in which KCl was reduced to 8 mM and 127 mM potassium gluconate was added, was used to check for spontaneous or multispike activity (Beutner & Moser 2001; Kawai *et al.* 2001). The mean chord conductances were calculated from the currents adjusted for driving force, assuming a Na^+ reversal potential of +56 mV. This value was estimated by applying 1 ms voltage steps to −30 mV from holding potential −110 mV to fully activate I_{Na}, followed by 20 ms depolarizations from −80 to +70 mV in 10 mV increments. Relative activation and inactivation curves of I_{Na} were best fitted with single Boltzmann function of the form $G/G_{max} = 1/(1 + \exp(V_{½} - V)/k$ for activation and $G/G_{max} = 1/(1 + \exp(V - V_{½})/k$ for inactivation where G was the electrical conductance, $V_{½}$ was half-activation or inactivation potentials and k the slope factor. Time constants for activation and inactivation were best fitted with single exponential functions of the form $A(1 - \exp(-t/\tau))$ for activation and $A(\exp(-t/\tau))$ for inactivation, where t was the time, A was the peak current and τ the exponential time constant for activation or inactivation. In the current-clamp configuration, depolarizing currents were applied in 10 or 50 pA steps up to 700 pA. TTX (100 nM, Sigma) was applied to the vicinity of the recorded hair cell through a large diameter pipette using a peristaltic pump. All experiments were conducted at room temperature. Data are given as means ± S.D.

Single-cell RT-PCR

Considering the utricular maculae's ultrastructure and close connections between heterogeneous populations of cells and post-synaptic fibres, we developed a strategy allowing us to detect simultaneously on single utricular hair cells several TTX-sensitive Na^+ channel isoforms, Nav1.1, Nav1.2, Nav1.3, Nav1.6 and Nav1.7, which are known to be expressed in the nervous system (Goldin, 1999). Single-cell harvesting and RT-PCR were performed as described by Lambolez *et al.* (1992). Patch pipettes were filled with 8 μl of the internal solution. The cellular content of individual

Table 1. Primer sequences and positions, length of PCR products and Genbank accession numbers of genes

Gene	Position	Sequence (5′–3′)	Product length (bp)	Accession no.
Nav com	—	ATCTTCATCATCTTCGGCTC	590	—
		AAAGAGCAGAGTGCGGATC		
Nav1.1	4649–4668	CATCATCTTCGGCTCGTTCT	316	X03638
	4943–4964	GCTTGTCACATAATCGCTCTGG		
Nav1.2	4583–4602	TCTTCGGCTCATTCTTCACC	311	X03639
	4871–4893	GTTGGTCATCTCCTGACTCTGGT		
Nav1.3	4763–4782	CGGCTCAAAGAAACCTCAGA	305	Y00766
	5048–5067	TCGAGAGAATCACCACCACA		
Nav1.6	4362–4381	GTTCATCGGTGTCATCATCG	355	L39018
	4697–4716	CAAGGCAAACATTTTGAGCA		
Nav1.7	4321–4340	TTCGGCTCATTCTTCACGTT	359	AF000368
	4660–4679	CACTCCCCAGTGAACAGGAT		
β–Actin	1547–1566	CACGGCATTGTAACCAACTG	288	V01217
	2279–2298	ACCCTCATAGATGGGCACAG		

hair cells was harvested under microscopic observation after obtaining a good seal and special care was taken to avoid contamination with adjacent cells or with the external bathing solution. The continuous perfusion of the utricular explant prevented the accumulation of contaminating material. The cellular content was expelled into a test tube and RNA was transcribed into cDNA by adding 3.5 μl of a mixed solution containing 5 μM of hexamer random primers (Boehringer Mannheim), 0.5 mM of each dNTP (Pharmacia), 10 mM of dithiothreitol, 20 U of recombinant RNase inhibitor (Promega, France) and 100 U of Superscript II reverse transcriptase (Invitrogen). The tube was then incubated at 37 °C overnight. Amplification was performed in two rounds of PCR. All of the RT product was used as a template for the first PCR with 0.1 μM of each primer, 10 × PCR buffer, 50 μM of dNTP and 2.5 U of HotStar Taq DNA polymerase (Quiagen) in a 100 μl final volume. The PCR reaction consisted of an initial activation step at 95 °C for 15 min, 40 cycles at 94 °C for 1 min, 55 °C for 1 min and 68 °C for 1 min followed by a final extension at 68 °C for 8 min (Hybaid Thermocycler). This first round of amplification was performed by using oligonucleotides (Nav com), fully matching the five TTX-sensitive Na^+ α-subunits (Nav1.1, Nav1.2, Nav1.3, Nav1.6 and Nav1.7) in a co-amplification with oligonucleotides for β-actin. Nav com was selected on regions of homology between segment S6 of domain III and segment S4 of domain IV. The simultaneous amplification of the different related gene members was designed to maintain the initial proportions of their mRNA. The concomitant β-actin amplification was used as a positive control for cell aspiration and subsequent RT-PCR efficiency, allowing us to remove undesirable samples. The second round of amplification was performed on 0.25 μl of the first amplification reaction as a template in a 50 μl final volume. This amplification was carried out to determine the molecular identity of the five isoforms simultaneously amplified during the first PCR round. Amplification was performed in separate tubes by using nested or semi-nested primers which specifically matched each of the five sodium α-subunit isoforms investigated. The amplification was as described above and for 32 cycles at an annealing temperature of 59 °C. Positive controls using total RNA from rat utricle or brain at early post-natal ages and negative controls using internal solution, external solution removed from bath, water or RNA without reverse transcriptase were simultaneously performed. Primer sequences are detailed in Table 1. All the primers used were designed to theoretically span exon–intron boundaries. This was confirmed by control amplifications performed on genomic DNA. The specificity and sensitivity of each primer used were carefully determined on as small an amount as 10 pg of total RNA. The identity of PCR products was confirmed at least one time by direct sequencing (Genome Express, France) and routinely by restriction enzyme analyses according to the manufacturer's protocol. The following restriction enzymes were used: *Taq* I, *Ban* II (Promega) *Aci* I, *Bsm* FI and *Ava* II (New England Biolabs). Predicted restriction fragments are detailed in Fig. 2*C*2.

Immunocytochemistry

Utricular maculae from P0–P3, P10 and P20 rats were fixed in 4 % paraformaldehyde in a 0.1 M phosphate-buffered saline (pH 7.4) for 2 or 12 h according to the developmental stage. Immunocytochemistry was carried out on free-floating sections (70 μm) which were permeabilized for 1 h 30 min in Tris buffer containing 0.2 % Tween 20, 0.1 % Triton X-100 and 10 % swine serum to reduce non-specific immunolabelling. Double immunostaining was performed by coincubation overnight at 4 °C with anti-Na^+ channel type II antibody, which specifically recognizes Nav1.2 α-subunit (1:20; Upstate Biotechnology) and a monoclonal anti-neurofilament 200 directed against the neurofilament heavy chain (1:500; Sigma). After rinsing, sample sections were exposed overnight at 4° to biotinylated anti-rabbit IgGs (1:400; Jackson ImmunoResearch Labs), then incubated with streptavidin Cy3-conjugated (1:500; Jackson ImmunoResearch Labs) and fluorescein-isothiocyanate-conjugated anti-mouse IgGs (Jackson ImmunoResearch Labs). For BDNF immunolabelling, utricular maculae were processed as previously described (Montcouquiol *et al.* 1998). Sections were mounted in Mowiol medium 4-88 (Calbiochem Corp., La Jolla, CA, USA) and observed with a Bio-Rad MRC 1024 laser scanning confocal microscope equipped with an ×40 oil immersion lens. Omitting the primary antibody incubation step routinely checked the specificity of immunostaining. Whatever the age studied, controls showed no specific fluorescence when primary antibodies were omitted (data not shown).

Analysis of BDNF levels

The levels of BDNF protein in culture media were measured by using the BDNF Emax immunoassay kit (Promega, Charbonnieres, France) in an antibody sandwich format as described by the manufacturer. In order to improve its sensitivity, we used a modification of the conventional ELISA methodology termed ELISA-*in situ* described by Balkowiec & Katz (2000), (see also Boukhaddaoui *et al.* 2001). Briefly, after dissection, P0 and P20 rat utricles were plated at five utricles per well, onto the anti-BDNF-coated wells (96 wells, Nunc MaxiSorp Polylabo, Strasbourg, France). Two hours after seeding, utricles were or were not stimulated for 60 min using 10 s trains of voltage pulses (3 ms duration, 9 V, 1 Hz) delivered every 10 s (GRASS S88 stimulator) in the presence or the absence of TTX. Both electrodes were T-shaped in a way that the length of their horizontal distal part facing the utricle covered the entire edge of the epithelium (about 500 μm). To ensure a reproducible electrical field across the utricle, both the neutral and the active electrodes were placed in both sides of the utricle at a similar distance (about 500 μm) from the epithelium. Stimulation protocols were chosen for their ability to induce reproducible transient intracellular Ca^{2+} increases in cultured DRG neurons loaded with the Ca^{2+}-sensitive dye fura-2 (data not shown). After stimulation, the plates were extensively washed to remove all cells. Wells were controlled with bright-field microscopy to ensure cell elimination. The subsequent steps were carried out according to the manufacturer's protocol. The amount of BDNF was quantified relative to a standard curve generated with known amounts of BDNF. The threshold of BDNF of detection was 10 pg ml^{-1}. Each experiment was repeated three times. Statistical significances were examined using the non-parametric Kruskall-Wallis test (Snedecor & Cochran, 1989).

RESULTS

Early post-natal utricular hair cells express neuronal-like TTX-sensitive voltage-gated Na^+ channels

Fast activating and voltage-dependent inactivating inward current was recorded in response to membrane depolarization from a holding potential of −110 mV in utricle hair cells of P0–P2 rats. Figure 1*A* shows a representative whole-cell current recorded in external control solution with a prominent depolarization-activated inward current. The current activated from a threshold of −60 mV peaked around −30 mV and then diminished in size linearly with increasing voltage steps, reaching zero current above +50 mV. Figure 1*B* illustrates the pharmacological block of this current using 100 nM TTX, a specific inhibitor of voltage-gated Na^+ channels. The inward current also disappeared when external Na^+ was substituted for equimolar choline (not shown). Altogether, these data indicated that the current was carried by Na^+ ions through neuronal-like TTX-sensitive Na^+ channels. Studying the Na^+ current (I_{Na}) in isolation revealed a mean time constant for activation ranging from 1.02 ± 0.14 ms at −55 mV to 0.11 ± 0.03 ms at +15 mV for a sample of seven hair cells. Steady-state inactivation was also voltage dependent. The time constant for inactivation ranged from 4.93 ± 1.04 ms at −55 mV to 0.26 ± 0.03 ms at +15 mV for a sample of 10 hair cells (Fig. 1*C–D*). In all cases, I_{Na} was completely inactivated within 7 ms. The mean half-activation and inactivation potentials were −39.0 ± 7.2 mV ($n = 16$) and −80.1 ± 9.6 mV ($n = 7$) respectively (Fig. 1*E–F*). These results indicate that at the resting potential (around −70 mV) 30 % of the Na^+ channels are available for activation. The properties of I_{Na} did not significantly vary when Ca^{2+} ions were removed from the control solution (not shown).

Single utricular hair cells co-express multiple α-subunit isoforms of voltage-gated Na^+ channels

The molecular characterization of the voltage-gated channels involved in the Na^+ conductance recorded was done by single-cell RT-PCR in two rounds of PCR amplification followed by restriction mapping on the cellular content of P1–P3 hair cells. The first co-amplification was performed on the reverse transcribed product by using a primer set, Nav com, fully matching conserved regions of the five α-subunits investigated in addition with β-actin primers (data not shown). The second amplification used specific primers for each Na^+ channel isoform detailed in Table 1. Figure 2*A* illustrates a coupling of an electrophysiological recording and a molecular investigation for a P3 utricle hair cell. After establishing the whole-cell configuration, I_{Na} could be visualized at fast time scale (Fig. 2*A*, inset). A negative pressure was then applied to the patch pipette and the intracellular content was harvested and subjected to molecular analysis (Fig. 2*B*). Single-cell RT-PCR analysis revealed the simultaneous expression of three subunits, Nav1.2, Nav1.3 and Nav1.6. Examples of the expression profiles obtained on four P1–P2 hair cells without prior recording are presented in Fig. 2*C*1. Each of these cells expressed multiple α-subunit isoforms. Patterns of expression from cell to cell were highly heterogeneous and illustrated well the high diversity of profiles – nine different profiles – found on the 13 cells analysed. Each of the five investigated isoform mRNAs was detected at least once. Direct sequencing of PCR products confirmed the molecular identity of each subunit. Specific restriction enzymes for individual subunits were routinely used giving restriction fragments of the predicted sizes as shown in Fig. 2*C*2. Control experiments performed on internal solution or external medium gave no specific amplification products in either the first or the second step of amplification (data not shown).

Considering the relative frequency of each mRNA expression, different levels were found from cell to cell (Fig. 2*D*). Two subunit mRNAs displayed a major expression, Nav1.2 (53.8 %) and Nav1.6 (76.9 %). These subunits were expressed either alone or in association with the others. Lower expression levels were found for the other subunits, Nav1.7 (30.8 %), Nav1.3 (23.1 %), with the lowest percentage of expression for Nav1.1 transcripts found in only one cell (7.7 %).

Early post-natal utricle hair cells are able to generate TTX-sensitive action potential

To test whether the occurrence of I_{Na} in the utricle hair cells may underlie the generation of action potentials, tight-seal whole-cell recording of the membrane potential was undertaken using the current-clamp configuration of the patch-clamp technique in P1 utricle hair cells. Their mean resting membrane potential was −70.04 ± 5.4 mV (n = 27). In this cell population, spontaneous generation of action potentials was not seen using either the control or low Cl^- internal solutions. However the injection of depolarizing currents in the range of those that would be carried by

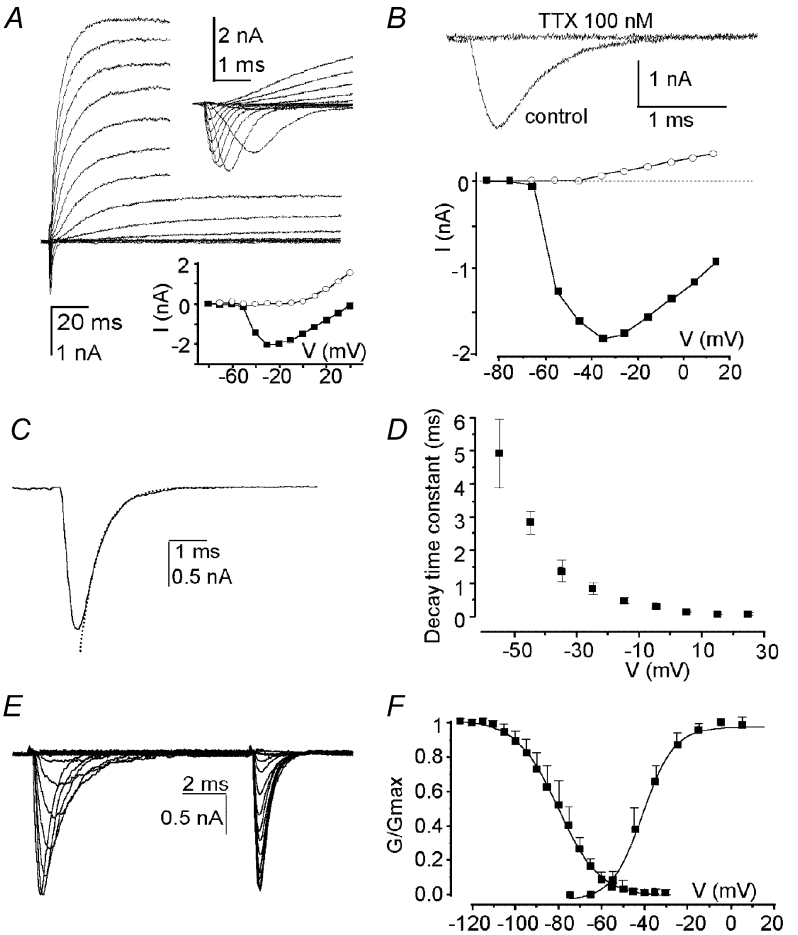

Figure 1. Early post-natal utricular hair cells express neuronal-like TTX-sensitive voltage-gated Na⁺ channels

A, voltage-activated whole-cell currents evoked in a post-natal day (P)1 hair cell in response to 10 mV incrementing depolarizing voltage steps between −80 and +50 mV from a holding potential (V_H) of −90 mV (residual (r) series resistance (R_s) 1.1 MΩ, membrane capacitance (C_m) 5.8 pF). Upper inset, fast time scale observation of the transient inward current evoked from a V_H of −112 mV. Bottom inset, plot of current amplitudes taken either at the peak of the inward current (■) or 5 ms after the beginning of the test pulse (○), as a function of the test potential for the hair cell shown. *B*, current traces illustrating the activation of pharmacologically isolated Na^+ current (I_{Na}) upon depolarization to −5 mV from a V_H of −112 mV in a P1 utricle hair cell and its block in presence of 100 nM TTX in the preparation. Bottom, plot of current amplitudes taken at the peak of the inward current before TTX application (■) or 1 ms after the beginning of the test pulse (○) after TTX application, as a function of the test potential. *C* and *D*, illustration of the fit with single exponential function (dashed line) of the decreasing phases of I_{Na} induced in isolation by 10 ms depolarizing pulses to −25 mV from a V_H of −115 mV (*C*), and plot of the mean decay time constant as a function of the test potential for a sample of 10 hair cells (*D*). *E* and *F*, traces illustrating the steady-state inactivation of I_{Na} using the following protocol (*E*): 5 ms depolarizing pulses to −25 mV were preceded by 10 ms conditioning prepulses from −125 to −20 mV from a V_H of −115 mV (rR_s 2.1 MΩ, C_m 5.2 pF), and plot of relative activation and inactivation of pharmacologically isolated I_{Na} expressed as G/G_{max}, where G is electrical conductance, as a function of test potential and conditioning prepulses respectively (*F*). Slope factors for the Boltzmann functions were 7.2 and 9.6 for the activation and the inactivation respectively. In *A*, *B*, *C* and *E*, residual capacitive transients were removed off-line. Traces shown throughout the figure are single traces.

mechanosensitive transduction channels (up to 700 pA) were able to trigger action potentials ($n = 17$). Figure 3 illustrates both voltage responses and the underlying whole-cell currents obtained in representative P1 hair cells. When the best current-clamp conditions were achieved and with a I_{Na} density higher than 4 nS pF^{-1}, spiking behaviour could be evoked with a mean current of (123.7 ± 75.8 pA $n = 9$) and with minimum current injection of 50 pA (Fig. 3*A*). Hair cell hyperpolarization improved the occurrence of action potentials by increasing their size as expected since more channels were recruited (Fig. 3*B*). The presence of TTX in the bathing solution reversibly prevented the occurrence of action potentials (Fig. 3*B*). Action potentials were also recorded in P0 and P2 hair cells, but not at other post-natal ages, excepted in one hair cell from a P10 utricle that was exceptional in displaying a current density close to 3 nS pF^{-1}. Multiple action potentials were not observed either for larger current injections or when low Cl^- internal solution was used. These data suggest that neuronal-like Na^+ channels are able to generate Na^+-driven TTX-sensitive action potentials in early post-natal utricle hair cells.

Voltage-gated Na^+ channels expression is developmentally regulated

We next analysed whether Na^+ channel expression is developmentally regulated. The temporal pattern of I_{Na} occurrence within hair cells was first examined by plotting the percentage of cells that express I_{Na} as a function of the day of development (Fig. 4*A*). Recordings taken every day from E20 to P8 and at P21 indicate that the expression of I_{Na} is tied to perinatal development. The percentage of cells exhibiting I_{Na} increased from 47 % at E20 ($n = 15$) to 93 % at P1 ($n = 14$), and then decreased to 81 % at P2 ($n = 49$), 75 % at P3 ($n = 8$) and 13 % at P8 ($n = 23$). After 3 weeks of development (P21), very small amplitude I_{Na} have been detected in only three out of the 59 adult hair cells examined. The density of I_{Na} in hair cells, obtained by dividing G_{max} by

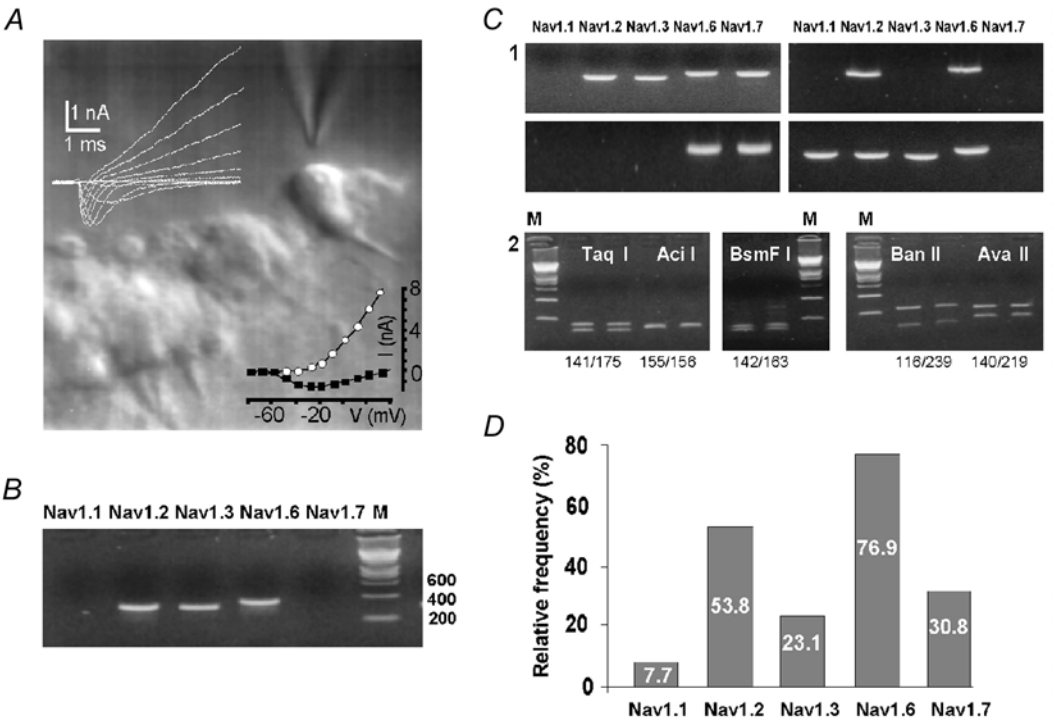

Figure 2. Molecular characterization of the Na^+ channels expressed by single utricle hair cells

A, Nomarski micrograph of a utricle hair cell. The recording electrode, of which only the tip is in focus, approaches the basolateral part of an exposed cell. Upper inset, fast time scale observation of the whole-cell current showing I_{Na} recorded following the protocol described in Fig. 1 (rR_s 1.3 MΩ, C_m 6.9 pF). Bottom inset, plot of current amplitudes taken either at the peak of the inward current (■) or 5 ms after the beginning of the test pulse (○), as a function of the test potential for the hair cell shown. *B*, agarose gel electrophoresis of single-cell RT-PCR products obtained after the second round of amplifications using specific primers for Na^+ channel α-subunits (Nav1.1, Nav1.2, Nav1.3, Nav1.6, Nav1.7) for the P3 cell recorded in *A*. Products were resolved with SmartLadder (Eurogentec) as a molecular weight marker (M). *C*1, expression profiles recovered from four P1–P2 cells showing a high diversity of expression profiles from cell to cell. *C*2, validation of the sequence identity of Nav1.1, Nav1.2, Nav1.3, Nav1.6 and Nav1.7 is demonstrated by expected restriction fragments sizes obtained by using specific restriction enzymes, *Taq* I, *Aci* I, *Bsm* F1, *Ban* II and *Ava* II for each of the five isoforms respectively. *D*, relative frequency expressed in percent of each Na^+ α-subunit mRNA in the 13 cells analysed between P1 and P3.

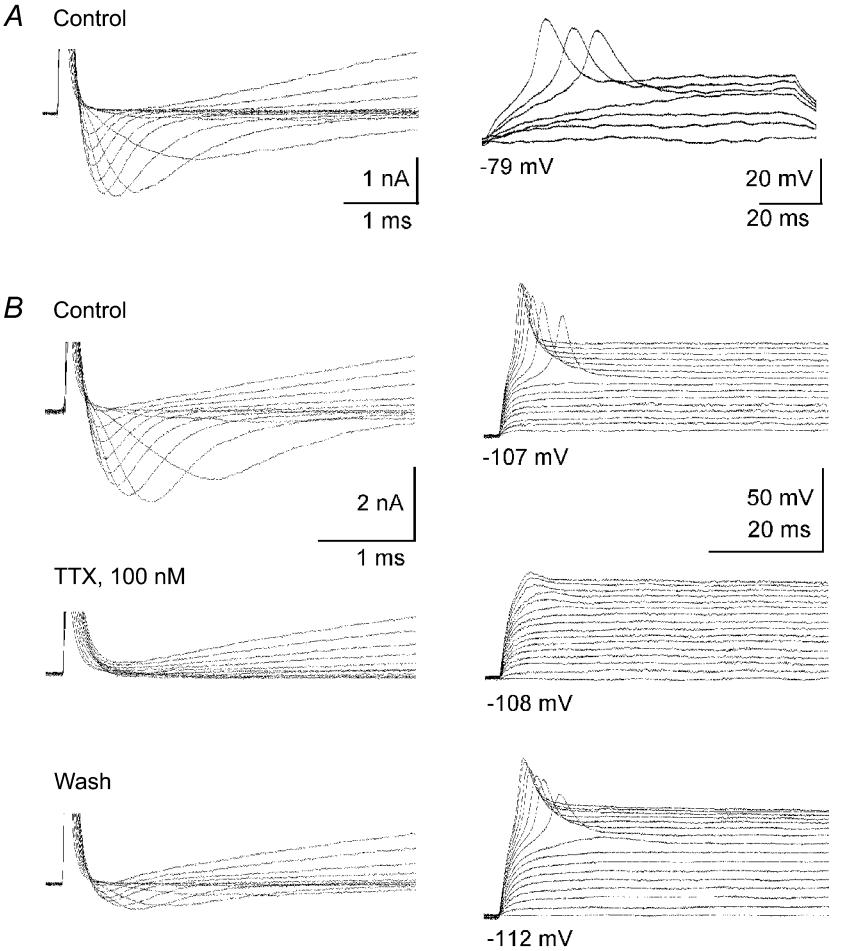

Figure 3. TTX-sensitive action potentials in response to current injections in early post-natal utricle hair cells

Voltage responses (right traces) recorded using the current-clamp mode of the patch-clamp technique, and their underlying whole-cell current (left traces) recorded using the voltage-clamp mode of the patch-clamp technique, following the protocol described in Fig. 1. Depolarizing current injections were applied in 10 pA (*A*) and 50 pA (*B*) steps either without (*A*) or under (*B*) application of hyperpolarizing holding current. *B*, traces were obtained in control solution, during TTX perfusion and after 15 min washing. Recording pipettes were filled with the low Cl^- solution in *A* and with the control internal solution in *B*. Traces shown throughout the figure are single traces. Data shown in *A* and *B* were obtained in P1 utricle hair cells.

the hair cell membrane capacitance, displayed a similar temporal pattern indicating that both the number of positive cells and the density of the current were maximal at P1 (Fig. 4*B*).

The transient expression of Na^+ channels was confirmed at protein level. Indeed, we investigated by the cellular localization of the Nav1.2 subunit, one of the most expressed isoforms, in the course of post-natal development. As shown in Fig. 5*Ba*, at early stages of development, Nav1.2 immunoreactivity appeared as dotted lines delineating hair cell membranes and some supporting cell basal membranes. It appeared as a strong staining along the apical part of the vestibular epithelium involving the apical cellular compartment of both hair cells and supporting cells (Fig. 5*Ba*). From P10 stage, a few hair cells were found labelled at their base with anti-Nav1.2 antibodies. At this time, Nav1.2 immunostaining was mainly detected along supporting cells length with a particularly sustained labelling of their basal intra-

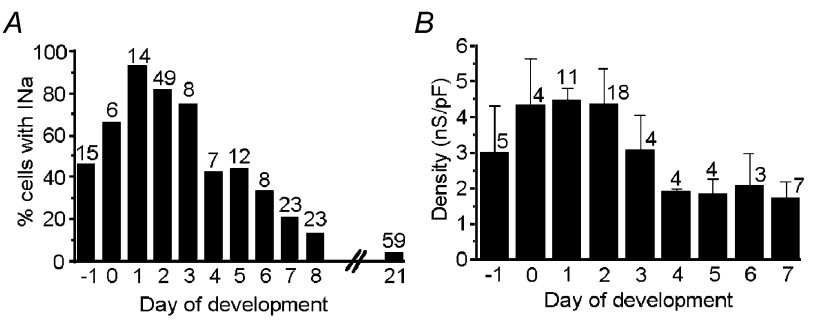

Figure 4. Transient expression of the voltage-gated Na^+ channels

A, diagram showing the percentage of hair cells exhibiting I_{Na} as a function of the day of development. *B*, diagram showing the density of I_{Na} as a function of the day of development. Only hair cells that expressed I_{Na} were included in the calculation of the current densities. In *A* and *B*, the number of cells studied at each stage of development is reported at the top of each column.

cellular compartment (Fig. 5*Bb*). The mature epithelium was characterized by the quasi-disappearance of sensory cell staining, while Nav1.2 immunoreactivity remained strongly present in the basal cellular compartment of supporting cells (Fig. 5*Bc*). Immunohistochemical and electrophysiological data strongly suggest that I_{Na} expressed by hair cells and their correlated spiking behaviours were restricted to the first post-natal week of development.

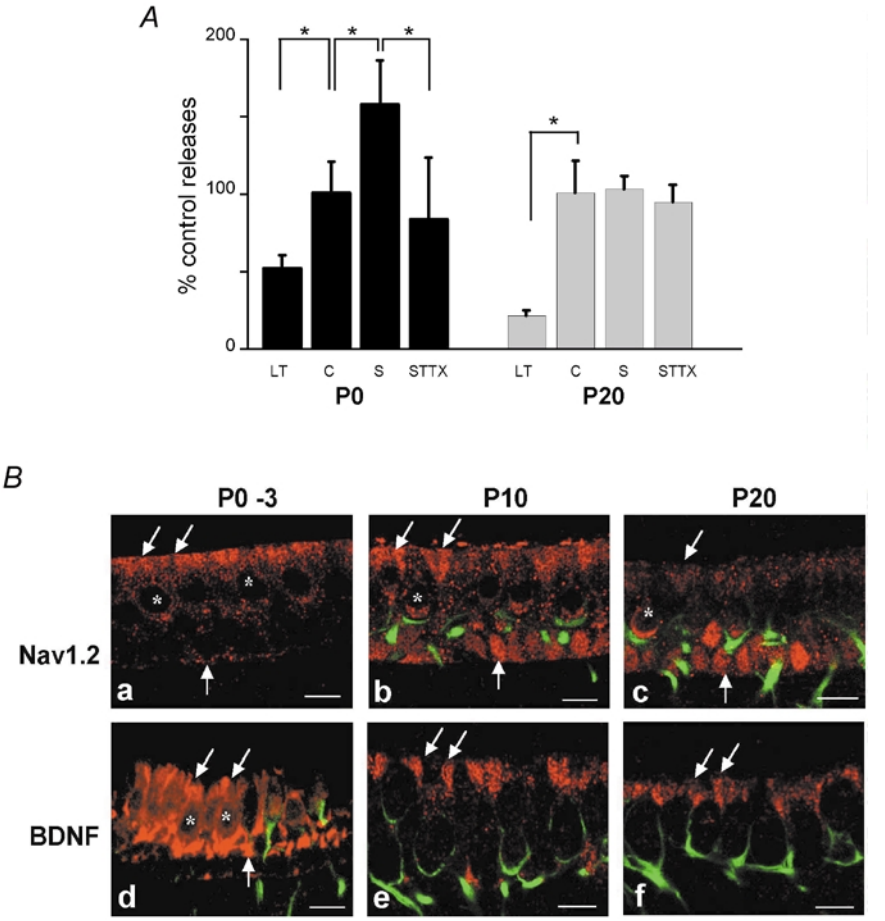

Figure 5. Activity-dependent BDNF release and developmental evolution of Nav 1.2 and BDNF immunoreactivities

A, TTX-sensitive activity-dependent brain-derived neurotrophic factor (BDNF) secretion during neonatal development. Diagram shows BDNF secretion, expressed as percentage of control secretions at P0 (black bars) and P20 (grey bars) from rat utricles at low temperature (LT) and control (C) conditions, under an electrical stimulation protocol in absence (S) or presence of TTX (STTX) in the bathing solution. Each column represents the mean of three experiments (±S.D.). Statistically significant differences are indicated by asterisks: * $P < 0.05$. *B,* developmental evolution of Nav1.2 and BDNF immunoreactivities. Laser confocal microscopy micrographs of double immunofluorescence staining using antibodies directed against Nav1.2 Na^+ channel subunit (*a–c*) or BDNF (*d–f*), (red labelling) and neurofilament (green labelling) at three developmental stages P0–3, P10 and P20. *Ba*, at early stages P0–P3, most of the neonatal hair cell (asterisks) membranes are immunostained with anti-Nav1.2 Na^+ channel antibodies. In addition, a strong level of staining within the apical part of the epithelium involving both hair cells and supporting cells is clearly identified (upper arrows). Some basal membranes of supporting cells (lower arrow) are also labelled. *Bb*, at P10, Nav1.2 immunostaining is detected in few sensory cells (asterisk), while it is intensely recovered within the apical region and the basal intracellular compartment of supporting cells (upper and lower arrows). *Bc*, in the mature utricular sensory epithelium (P20), Nav1.2 immunoreactivity is mainly restricted to the basal intracellular compartments of supporting cells (arrows). Sensory cells are devoid of immunostaining except for isolated cells (asterisk) remaining labelled. *Bd*, the cytoplasm of hair cells (asterisks) and the middle part of supporting cells (arrow) display a strong BDNF immunostaining at neonatal stages. *Be* and *f*, from P10 stage, BDNF immunoreactivity is no longer detected in sensory cells and appears as restricted to the apex of supporting cells (upper arrows). Neurofilament co-staining (green labelling) shows the epithelium innervation. Calyceal endings of afferent fibres innervating type I sensory cells are clearly identified. Scale bar = 10 μm.

Activity-dependent BDNF release in early post-natal utricle explants

Since activity-dependent release of neurotrophin controls important aspects of neuronal development and plasticity in the nervous system, we next addressed whether Na^+ channels could also regulate an activity-dependent secretion of BDNF by hair cells during the post-natal period. Using a highly sensitive ELISA assay (ELISA *in situ*) (Balkowiec & Katz, 2000), utricle secretion of BDNF was compared following 60 min of either control conditions or electrical stimulation in the presence or absence of 1 μM TTX (Fig. 5*A*). BDNF released by the utricle in control conditions was 35 ± 7 pg ml^{-1} ($n = 3$) at P0 and 82 ± 17 pg ml^{-1} ($n = 3$) at P20. Electrical stimulation increased BDNF release by about 60 % (55 ± 10 pg ml^{-1}) of the control value in the P0 utricles ($P < 0.05$), whereas it had no effect on BDNF secretion (84 ± 7 pg ml^{-1}) in the P20 utricles. In the presence of TTX, the effect of electrical stimulation was abolished in P0 utricles since BDNF release remained at control level (29 ± 14 pg ml^{-1}; $n = 3$). At P20, TTX had no consequence on BDNF secretion (77 ± 9 pg ml^{-1}; $n = 3$). Constitutive release was evaluated by lowering the temperature down to 15 °C to block protein transport from the endoplasmic reticulum to the Golgi structure. This significantly ($P < 0.05$) diminished the basal level of BDNF to about 50 % of the control release at P0 (18 ± 3 pg ml^{-1}; $n = 3$) and 20 % at P20 (17 ± 3 pg ml^{-1}; $n = 3$). These results are in accordance with the BDNF labelling of sensory cells and of supporting cells at birth, which becomes restricted to supporting cells at P21. As shown in Fig. 5*Bd* at early post-natal stages, BDNF labelling was detected in the cytoplasm of hair cells and was found to be intensely concentrated in the middle part of supporting cells just above the basal layer of the epithelium. From P10 stage, the absence of hair cell staining by anti-BDNF antibodies was manifest, whereas immunolabelling was mainly restricted within the apex of supporting cells (Fig. 5*Be* and *f*).

DISCUSSION

The main finding of this study was the observation that early post-natal vestibular hair cells express neuronal-like TTX-sensitive Na^+ channels able to generate Na^+-driven action potentials and to induce activity-dependent BDNF secretion. The causal link between the Na^+ channel activation, the generation of action potentials and the BDNF release was demonstrated by the finding that treatment by TTX – which specifically blocked a family of voltage-activated Na^+ channels – completely abolished the action potential induced by depolarization and the BDNF secretion induced by electrical stimulation. In the course of the maturation of the vestibular system, I_{Na} disappears from utricular hair cells during the second post-natal week and electrical stimulation fails to induce BDNF release.

Molecular analyses confirm that utricular sensory receptors express neuronal TTX-sensitive Na^+ channel isoforms. Our results demonstrate that several Na^+ channel α-subunits are expressed in single utricular hair cells in a heterogeneous way from cell to cell. The co-expression of multiple isoforms of voltage-gated Na^+ channels has been largely described in nervous tissues (Black *et al.* 1996; Felts *et al.* 1997; Fjell *et al.* 1997; Whitaker *et al.* 2000; Alessandri-Haber *et al.* 2002), but in mammals at the single-cell level in only a few reports (Vega-Saenz de Miera *et al.* 1997; Richardson *et al.* 2000). A phenotypic diversity from cell to cell has already been reported by single-cell experiments on multigene families including voltage-gated Na^+ channels (Plant *et al.* 1998; Cauli *et al.* 2000; Richardson *et al.* 2000). Here, hair cell developmental processes are known to be gradual and to show in addition regional variations (Sans & Chat 1982; Rusch *et al.* 1998). Therefore, at early post-natal ages, heterogeneous populations of hair cells may account for at least part of the phenotypic diversity observed. Any attempt to interpret conclusively on the physiological relevance of this multiple and heterogeneous expression will be premature because of the limitation of transcriptional studies which do not necessarily reflect a functional protein expression. Further studies will be needed to explore the exact contribution at the functional level of each subunit and especially the most expressed Nav1.2 and Nav1.6 subunits.

The Na^+ channel current that we describe here displays similar biophysical and pharmacological characteristics to those described for axonal I_{Na} (Hodgkin & Huxley, 1952; Moore *et al.* 1967): activation threshold, time constants for activation and inactivation, half-activation and inactivation potentials and sensitivity to TTX. These characteristics are consistent with its activation at resting potential upon slight depolarizing stimuli. These results differ from the previous observations on cultured mouse utricle hair cell preparations when inactivation properties of I_{Na} appeared to prevent any action potential at the resting membrane potential (Eatock & Rusch, 1997; Rusch & Eatock, 1997). Such discrepancies may be due to differences between species (mouse *vs.* rat). Since hair cells have been recorded from chronic organotypic cultures rather than from acute explants as in the present study, the Na^+ channel might have been differentially modulated by *in vitro* conditions.

From the steady-state inactivation curve, it appears that 30 % of Na^+ channels are available for activation at resting membrane potential at around −70 mV. The steady-state activation curve indicates that the Na^+ channels are not activated at the resting potential, but that slight depolarizations would be sufficient to open the channels with the consequence of speeding up membrane depolarization, and transmitter and BDNF release at the basal membrane of hair cells. Such a scenario has been

proposed in mammal retina bipolar cells, which are silent cells that also express I_{Na} (Pan & Hu, 2000). TTX-sensitive action potentials could be evoked upon injection of depolarizing current in the range of physiological stimuli, i.e. those that would be carried by mechanosensitive transduction channels (as low as 50 pA). *In vivo*, the vestibular system is already functional in neonatal rodents, since a significant transducer current was detected in the sensory hair cells of neonatal mice (Geleoc *et al.* 1997) and an evoked electrical activity was recorded in the vestibular nerve of neonatal rat after ampullar stimulation (Curthoys, 1982). This indicates that there is enough transducer current to induce a spiking activity. Therefore, it is likely that the evoked Na^+ channel activation reported in this study is physiologically relevant. The very large percentage of I_{Na} expression between P0 and P2 hair cells together with its almost total loss (there is only occasional expression of small I_{Na} in some adult hair cells) in the two types of hair cells along with the maturation process suggest that I_{Na} could be a marker of the hair cell immaturity.

Another important finding of this study is the observation that Na^+ channel activation controls BDNF release induced by utricular hair cell electrical stimulation. These data extend for the first time to a non-neuronal sensory receptor, the previously described activity-dependent neurotrophin release in the nervous system (Thoenen, 1995). Activity-dependent BDNF release by utricular hair cells is restricted to the post-natal developmental period. During the same developmental period and before mature sensorineural synaptogenesis, mouse cochlear hair cells express NT3 and probable contributions of Na^+ currents to spiking activity have been reported in a number of vertebrate auditory hair cells (Evans & Fuchs, 1987; Kros *et al.* 1998). These cells also display spontaneous Ca^{2+}-driven action potentials (Kros *et al.* 1998; Beutner & Moser, 2001). This spontaneous spiking activity then disappears with the increase in size of the potassium current (I_{Kl}) that hyperpolarizes the cells (Marcotti *et al.* 2003). The regulated neurotrophin secretion that we observed in vestibular hair cells may be representative of a broader phenomenon for non-neuronal peripheral sensory receptors, especially in the inner ear.

The activation of Na^+ channels may be of functional importance during the vestibular system maturation and differentiation. Almost all early post-natal hair cells express Na^+ channels whose activation induces Na^+-driven action potentials and activity-dependent BDNF release. During this period, BDNF plays an important role in the survival of vestibular ganglion neurons and the establishment of sensory synapses (Ylikoski *et al.* 1993; Ernfors *et al.* 1995; Shimmang *et al.* 1995). BDNF is expressed by hair cells and supporting cells during the first 3 post-natal days in rats and its expression becomes highly compartmentalized and limited to supporting cells in the mature stages (Montcouquiol *et al.* 1998). Beside the Na^+-based activity-dependent BDNF release that occurs during the first post-natal days, BDNF is also secreted constitutively. Only the constitutive release remains in the mature epithelium. Even if it cannot be excluded that supporting cells may participate in the activity-dependent BDNF release since their excitability has not been checked, our results suggest that sensory hair cells are directly implicated in the activity-dependent BDNF release, while supporting cells release BDNF through a constitutive pathway. The former mechanism could be implicated in the survival and the setting up of synapses between nerve fibres and hair cells while the latter acts to maintain the mature synapse.

In conclusion, the transient expression of neuronal-like Na^+ channels may represent an important functional feature of immature rat neonatal hair cells. Their activation appears to induce TTX-sensitive Na^+ influx and action potentials during the first post-natal days. In turn, this activity is able to control a TTX-sensitive BDNF secretion and probably also, release of neurotransmitters, the two main factors acting in synapse competition and stabilization that occur during this developmental period in the rat utricle epithelium.

REFERENCES

Alessandri-Haber N, Alcaraz G, Deleuze C, Jullien F, Manrique C, Couraud F, Crest M & Giraud P (2002). Molecular determinants of emerging excitability in rat embryonic motoneurons. *J Physiol* **541**, 25–39.

Balkowiec A & Katz DM (2000). Activity-dependent release of endogenous brain-derived neurotrophic factor from primary sensory neurons detected by ELISA in situ. *J Neurosci* **20**, 7417–7423.

Beutner D & Moser T (2001). The presynaptic function of mouse cochlear inner hair cells during development of hearing. *J Neurosci* **21**, 4593–4599.

Black JA, Dib-Hajj S, McNabola K, Jeste S, Rizzo MA, Kocsis JD & Waxman SG (1996). Spinal sensory neurons express multiple sodium channel alpha-subunit mRNAs. *Brain Res Mol Brain Res* **43**, 117–131.

Boukhaddaoui H, Sieso V, Scamps F & Valmier J (2001). An activity-dependent neurotrophin-3 autocrine loop regulates the phenotype of developing hippocampal pyramidal neurons before target contact. *J Neurosci* **21**, 8789–8797.

Cauli B, Porter JT, Tsuzuki K, Lambolez B, Rossier J, Quenet B & Audinat E (2000). Classification of fusiform neocortical interneurons based on unsupervised clustering. *Proc Natl Acad Sci U S A* **97**, 6144–6149.

Curthoys IS (1982). Postnatal developmental changes in the response of rat primary horizontal semicircular canal neurons to sinusoidal angular accelerations. *Exp Brain Res* **47**, 295–300.

Eatock RA & Rusch A (1997). Developmental changes in the physiology of hair cells. *Semin Cell Dev Biol* **8**, 265–275.

Ernfors P, Van De Water T, Loring J & Jaenisch R (1995). Complementary roles of BDNF and NT-3 in vestibular and auditory development. *Neuron* **14**, 1153–1164.

Evans MG & Fuchs PA (1987). Tetrodotoxin-sensitive, voltage-dependent sodium currents in hair cells from the alligator cochlea. *Biophys J* **52**, 649–652.

Felts PA, Yokoyama S, Dib-Hajj S, Black JA & Waxman SG (1997). Sodium channel alpha-subunit mRNAs I, II, III, NaG, Na6 and hNE (PN1): different expression patterns in developing rat nervous system. *Brain Res Mol Brain Res* **45**, 71–82.

Fjell J, Dib-Hajj S, Fried K, Black JA & Waxman SG (1997). Differential expression of sodium channel genes in retinal ganglion cells. *Brain Res Mol Brain Res* **50**, 197–204.

Fritzsch B, Maklad A, Bruce LL & Crapon de Caprona MD (2001). Development of the ear and of connections between the ear and the brain: is there a role for gravity? *Adv Space Res* **28**, 595–600.

Fritzsch B, Silos-Santiago II, Bianchi LM & Farinas II (1997). Effects of neurotrophin and neurotrophin receptor disruption on the afferent inner ear innervation. *Semin Cell Dev Biol* **8**, 277–284.

Geleoc GS, Lennan GW, Richardson GP & Kros CJ (1997). A quantitative comparison of mechanoelectrical transduction in vestibular and auditory hair cells of neonatal mice. *Proc R Soc Lond B Biol Sci* **264**, 611–621.

Ghosh A, Carnahan J & Greenberg ME (1994). Requirement for BDNF in activity-dependent survival of cortical neurons. *Science* **263**, 1618–1623.

Goggi J, Pullar IA, Carney SL & Bradford HF (2002). Modulation of neurotransmitter release induced by brain-derived neurotrophic factor in rat brain striatal slices *in vitro*. *Brain Res* **941**, 34–42.

Goldin AL (1999). Diversity of mammalian voltage-gated sodium channels. *Ann N Y Acad Sci* **868**, 38–50.

Hodgkin AL & Huxley AF (1952). The dual effect of membrane potential on sodium conductance in the giant axon of Loligo. *J Physiol* **116**, 497–506.

Kafitz KW, Rose CR, Thoenen H & Konnerth A (1999). Neurotrophin-evoked rapid excitation through TrkB receptors. *Nature* **401**, 918–921.

Katz LC & Shatz CJ (1996). Synaptic activity and the construction of cortical circuits. *Science* **274**, 1133–1138.

Kawai F, Horiguchi M, Susuki H & Miyachi E (2001). Na^+ action potentials in human photoreceptors. *Neuron* **30**, 451–458.

Kros CJ, Ruppersberg P & Rusch A (1998). Expression of a potassium current in inner hair cells during development of hearing in mice. *Nature* **394**, 281–284.

Lambolez B, Audinat E, Bochet P, Crepel F & Rossier J (1992). AMPA receptor subunits expressed by single Purkinje cells. *Neuron* **9**, 247–258.

Lennan GW, Steinacker A, Lehouelleur J & Sans A (1999). Ionic currents and current-clamp depolarisations of type I and type II hair cells from the developing rat utricle. *Pflugers Arch* **438**, 40–46.

Marcotti W, Johnson SL, Holley MC & Kros CJ (2003). Developmental changes in the expression of potassium currents of embryonic, neonatal and mature mouse inner hair cells. *J Physiol* **548**, 383–400.

Montcouquiol M, Valat J, Travo C & Sans A (1997). Short-term response of postnatal rat vestibular neurons following brain-derived neurotrophic factor or neurotrophin-3 application. *J Neurosci Res* **50**, 443–449.

Montcouquiol M, Valat J, Travo C & Sans A (1998). A role for BDNF in early postnatal rat vestibular epithelia maturation: implication of supporting cells. *Eur J Neurosci* **10**, 598–606.

Moore JW, Blaustein MP, Anderson NC & Narahashi T (1967). Basis of tetrodotoxin's selectivity in blockage of squid axons. *J Gen Physiol* **50**, 1401–1411.

Neher E (1992). Correction for liquid junction potentials in patch clamp experiments. *Methods Enzymol* **207**, 123–131.

Pan ZH & Hu HJ (2000). Voltage-dependent Na^+ currents in mammalian retinal cone bipolar cells. *J Neurophysiol* **84**, 2564–2571.

Pirvola U, Arumae U, Moshnyakov M, Palgi J, Saarma M & Ylikoski J (1994). Coordinated expression and function of neurotrophins and their receptors in the rat inner ear during target innervation. *Hear Res* **75**, 131–144.

Pirvola U, Ylikoski J, Palgi J, Lehtonen E, Arumae U & Saarma M (1992). Brain-derived neurotrophic factor and neurotrophin 3 mRNAs in the peripheral target fields of developing inner ear ganglia. *Proc Natl Acad Sci U S A* **89**, 9915–9919.

Plant TD, Schirra C, Katz E, Uchitel OD & Konnerth A (1998). Single-cell RT-PCR and functional characterization of Ca^{2+} channels in motoneurons of the rat facial nucleus. *J Neurosci* **18**, 9573–9584.

Richardson PJ, Dixon AK, Lee K, Bell MI, Cox PJ, Williams R, Pinnock RD & Freeman TC (2000). Correlating physiology with gene expression in striatal cholinergic neurones. *J Neurochem* **74**, 839–846.

Rusch A & Eatock RA (1997). Sodium currents in hair cells of the mouse utricle. In *Diversity in Auditory Mechanics,* ed. Lewis ER, Long GR, Lyon RF, Steele CR, Narins PM & Hecht-Poinar E, pp. 549–555. World Scientific, Singapore.

Rusch A, Lysakowski A & Eatock RA (1998). Postnatal development of type I and type II hair cells in the mouse utricle: acquisition of voltage-gated conductances and differentiated morphology. *J Neurosci* **18**, 7487–7501.

Sans A & Chat M (1982). Analysis of temporal and spatial patterns of rat vestibular hair cell differentiation by tritiated thymidine radioautography. *J Comp Neurol* **206**, 1–8.

Schimmang T, Minichiello L, Vazquez E, San Jose I, Giraldez F, Klein R & Represa J (1995). Developing inner ear sensory neurons require TrkB and TrkC receptors for innervation of their peripheral targets. *Development* **121**, 3381–3391.

Snedecor GW & Cochran WG (1989). *Statistical Methods*, 8th edn. Iowa State University Press, Iowa, USA.

Stoop R & Poo MM (1996). Synaptic modulation by neurotrophic factors: differential and synergistic effects of brain-derived neurotrophic factor and ciliary neurotrophic factor. *J Neurosci* **16**, 3256–3264.

Thoenen H (1995). Neurotrophins and neuronal plasticity. *Science* **270**, 593–598.

Vega-Saenz de Miera EC, Rudy B, Sugimori M & Llinas R (1997). Molecular characterization of the sodium channel subunits expressed in mammalian cerebellar Purkinje cells. *Proc Natl Acad Sci U S A* **94**, 7059–7064.

Whitaker WR, Clare JJ, Powell AJ, Chen YH, Faull RL & Emson PC (2000). Distribution of voltage-gated sodium channel alpha-subunit and beta- subunit mRNAs in human hippocampal formation, cortex, and cerebellum. *J Comp Neurol* **422**, 123–139.

Ylikoski J, Pirvola U, Moshnyakov M, Palgi J, Arumae U & Saarma M (1993). Expression patterns of neurotrophin and their receptor mRNAs in the rat inner ear. *Hear Res* **65**, 69–78.

Acknowledgements

This work was supported by grant 793/01/CNES/8529/00. The authors want to thank Professor A. Touati for helpful advice in immunocytochemical studies, Doctor G. Lennan who took part in the electrophysiological recordings, Doctor S. Gaboyard who took part in the BDNF secretion experiments, Doctor P. Carrol for careful reading of the manuscript and C. Travo for excellent technical assistance.